



Article

Application of Multispectral Images from Unmanned Aerial Vehicles to Analyze Operations of a Wastewater Treatment Plant

Bartosz Szela^{1,*}, Szymon Sobura² and Renata Stoińska³¹ Department of Geotechnics and Waste Management, Kielce University of Technology, 25-314 Kielce, Poland² Department of Geodesy and Geomatics, Kielce University of Technology, 25-314 Kielce, Poland; ssobura@tu.kielce.pl³ Department of Water and Wastewater Technology, Kielce University of Technology, 25-314 Kielce, Poland; rstoinska@tu.kielce.pl

* Correspondence: bszelag@tu.kielce.pl

Abstract: The main task of a wastewater treatment plant (WWTP) is to reduce pollutants that adversely affect the receiving environment in which the effluent is discharged. The operation of a WWTP is a complex task due to the number of different processes that take place in its process facilities. In order to maintain the high efficiency of a WWTP, it is necessary to control the quality of the effluent at the outlet and monitor the processes taking place there. The main objective of the research presented in this study was to evaluate the possibility of using unmanned aerial vehicle (UAV) technology and multispectral images acquired with a Micasense Red-Edge MX camera to analyse the performance of an activated sludge bioreactor using the example of a municipal WWTP in Poland. Remote sensing analyses were carried out to check the relationships between the calculated spectral indices and the quality parameters in the bioreactor. The spectral indices assessed were the normalised difference vegetation index (NDVI), green normalised difference vegetation index (GNDVI), optimised soil adjusted vegetation index (OSAVI), and their derived indices, after substitution of the red or near-infrared channel with the red edge channel. In this study, the sensitivity of the NDVI and GNDVI_{RED-EDGE} indexes to changes in the nutrient content (NUC) of the bioreactor was observed. The presented research may find application in the design of a new soft sensor for monitoring the operating conditions of wastewater treatment plants.

Keywords: wastewater treatment plant (WWTP); unmanned aerial vehicle (UAV); spectral analyses; multispectral images; GNDVI (green normalised difference vegetation index)



Citation: Szela, B.; Sobura, S.; Stoińska, R. Application of Multispectral Images from Unmanned Aerial Vehicles to Analyze Operations of a Wastewater Treatment Plant. *Energies* **2023**, *16*, 2871. <https://doi.org/10.3390/en16062871>

Academic Editors: Katarzyna Bernat and Dorota Kulikowska

Received: 12 January 2023

Revised: 14 March 2023

Accepted: 15 March 2023

Published: 20 March 2023



Copyright: © 2023 by the authors. Licensee MDPI, Basel, Switzerland. This article is an open access article distributed under the terms and conditions of the Creative Commons Attribution (CC BY) license (<https://creativecommons.org/licenses/by/4.0/>).

1. Introduction

The main task of a wastewater treatment plant (WWTP) is to reduce pollutants that adversely affect the receiving environment in which the effluent is discharged. The operation of a WWTP is a complex task due to the number of different processes that take place in its process facilities [1,2]. In order to simplify and reduce the operating costs of the WWTP, it is advisable to determine the variability in raw wastewater quality at the design stage, which influences the selection of appropriate treatment technologies [3–5]. In order to achieve high effluent treatment efficiency, a process in individual bioreactor compartments is needed. Online analysers are installed in the bioreactor to measure selected wastewater quality indicators (WQI) to ensure treatment efficiency. However, because of the costs of their operation, i.e., energy consumption, reagents, and local conditions, their use is not always possible. For this reason, computational models are built at WWTPs using the data collected therein, using machine learning methods and thus creating so-called soft sensors. This solution allows for the modelling and control of wastewater treatment processes but requires input data to be provided to the model as a basis for performing simulation calculations [4]. As the quality of wastewater and its physicochemical characteristics change, measurement data may be subject to errors [6]. Additionally, these

sensors require calibration, so their use may be limited. With these problems in mind, high-resolution images taken with cameras and multispectral cameras are used to analyse the operation of WWTPs. These allow the microbiological composition to be identified and the quality of the wastewater to be determined. Literature [7–9] shows that spectral methods based on narrow spectral bands can also be used to identify effluent quality, but this approach has currently found applications for laboratory-scale analyses performed with synthetic wastewater. This solution seems to be interesting from the point of view of identifying the operating conditions of a WWTP, which in turn, could enable a rapid assessment of the conditions that occur in the individual compartments of a bioreactor. This problem has not yet been analysed on a larger scale, which is interesting given the relatively high agreement of the measurement results using spectral images [10].

The main objective of the research presented in this paper was to assess the possibility of using UAV technology and multispectral images acquired with the Micasense Red-Edge MX camera to analyse the performance of an activated sludge bioreactor on the example of a municipal WWTP in Poland. This study used a bioreactor that operates with activated sludge technology and consists of compartments for nitrification, denitrification, and dephosphatation. In order to verify the results obtained from the multispectral camera, measurements of the effluent quality indicators ammonium nitrogen ($\text{NH}_4\text{-N}$), phosphate ($\text{PO}_4\text{-P}$), and nitrate nitrogen ($\text{NO}_3\text{-N}$) were carried out in selected compartments of the bioreactor. Spectral curves and spatial maps of spectral indices in the form of NDVI, GNDVI, OSAVI, and derivatives of these indices were analysed for comparison.

UAV Applications in Wastewater Treatment Plants

In the review of the literature, several scientific studies related to the study of UAV technology can be found in the context of improving WWTP operations and water management. In the study [8], the authors conducted a number of UAV inspections to determine the deformation state of the floating cover over WWTP bioreactors in Australia, identifying a number of advantages over contact methods. In the study [10], the authors used multispectral data from UAVs as a decision-making tool to improve irrigation management in China. In [11], UAV technology was investigated in the context of reducing maintenance costs of wastewater treatment facilities. The proprietary algorithm developed for the study was able to identify resource failure with an accuracy of 55% to 81% for biological deposits and with an accuracy of 95% for failures related to activated sludge processes. This means that UAV imagery is able to help identify failures at WWTP sites and minimise the costs associated with maintaining some of the equipment found at the plant site. A derivative product of UAV data post-processing is a digital surface model (DSM), which, according to [12], can be used successfully to create hydrological models in treatment plant areas and urban areas for the analysis of drainage systems. However, it has not been possible to find many papers focussing on the use of multispectral images from UAVs in the context of their application to improve the operation of WWTPs and control the operation of bioreactors.

Significant developments in miniaturisation and advances in remote sensing imaging made in recent years are encouraging the application of new sensors under UAVs [13,14]. As a result, it is becoming possible to monitor and manage crops efficiently or supervise water facilities that require rapid response systems [15]. Remote sensing technologies adapted to flying UAV platforms are less susceptible to weather conditions than the use of satellite imagery for the same purpose. The high spatial resolution of UAV imagery, up to a few centimetres, allows for the detection of even small changes around the survey object being analysed [16,17]. Visual inspection of the object's condition by independent observers is not always feasible, especially for large-scale objects. In addition, visual assessment of the test object based on the visible spectrum of electromagnetic radiation does not always reveal all anomalies on the object. Increasing the number of spectral channels widens the range of interpretation possibilities, and hence the acquisition of hyperspectral images is becoming increasingly popular [14].

The variability of the spectral curve—the spectral response of an object (or phenomenon) as a function of electromagnetic wavelength—allows analyses to be carried out in a noncontact manner and is reflected in the variable values of spectral indices. The world literature has repeatedly focused on the variability of the spectral curve for vegetation, which shows a high instability in the red and infrared ranges of electromagnetic wavelengths, depending on the condition of the plant under study. There are many scientific papers in which the authors attempt to create rigorous mathematical models based on the correlation of spectral indices with the physical and chemical parameters under study [18]. Examples include models that closely relate the spectral response to heavy metal content in soil [19–21], nitrogen content in agricultural fields [18], or qualitative parameters that describe the status of describing surface water [22]. Such a large spectrum of applications encourages testing the potential of remote sensing imaging in other scientific disciplines than those cited earlier.

2. Study Area

A WWTP located in Starachowice, Świętokrzyskie Voivodeship, Poland, was selected as the test area for this study. The location of the testing ground is shown in Figure 1. There are two operational bioreactors at the plant, where analysers and probes have been installed to measure selected nutrient compounds in real time. The WWTP uses a system for the interlocked removal of nitrogen and phosphorus carbon compounds from wastewater as a three-stage Bardenpho system, otherwise known as A2/O. The three-stage Bardenpho is formed by compartments connected in series: anaerobic, aerobic, and oxygen compartments.

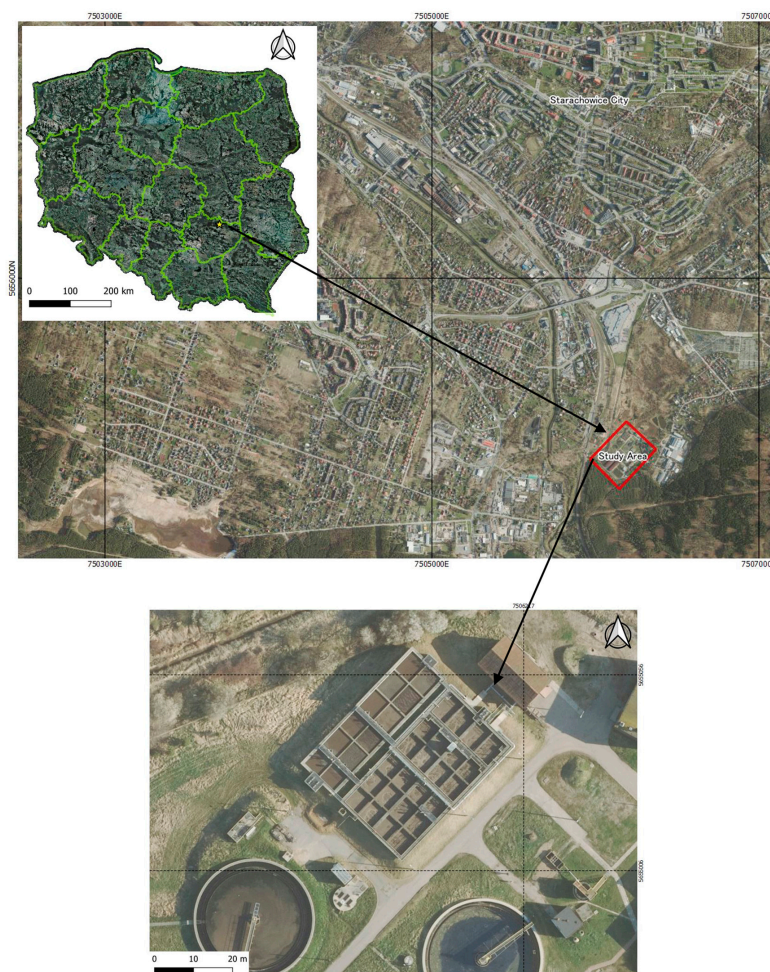


Figure 1. Location of the testing area in Starachowice (Poland).

The WWTP in question began operating in 1963 and receives wastewater discharged from the city of Starachowice. After modernisation in the 1980s, the hydraulic capacity of the plant was increased to 24,000 m³/d. The last modernisation of the WWTP was carried out between 2008 and 2011, during which all existing biological beds were decommissioned. The effluent of the secondary settling tanks is discharged into the Młynówka river. The indicated experimental facility was selected for this study due to problems with the correct operation of the bioreactors and their planned modernisation. Thus, the results of the research could find practical application in the implementation phase of the technology studied during the modernisation of the facility.

3. Methods

The research methodology adopted included carrying out a flight with an unmanned vehicle equipped with a multispectral camera, acquiring online data from sensors placed in the bioreactor, and conducting spectral analyses using spectral index maps. The following chapters provide a detailed description of the subsequent stages of the experiment.

3.1. UAV Flight

The measurement experiment was conducted on 6 April 2021. Three flights were carried out over the test field by different UAV platforms with different optical sensors. During the measurement day, there was total cloud cover of the sky, making it difficult to fly the UAV in global positioning system (GPS) mode. However, the weather conditions were positive in terms of registering the intensity of electromagnetic radiation. A schematic of the experimental work associated with the UAV is presented in Figure 2.

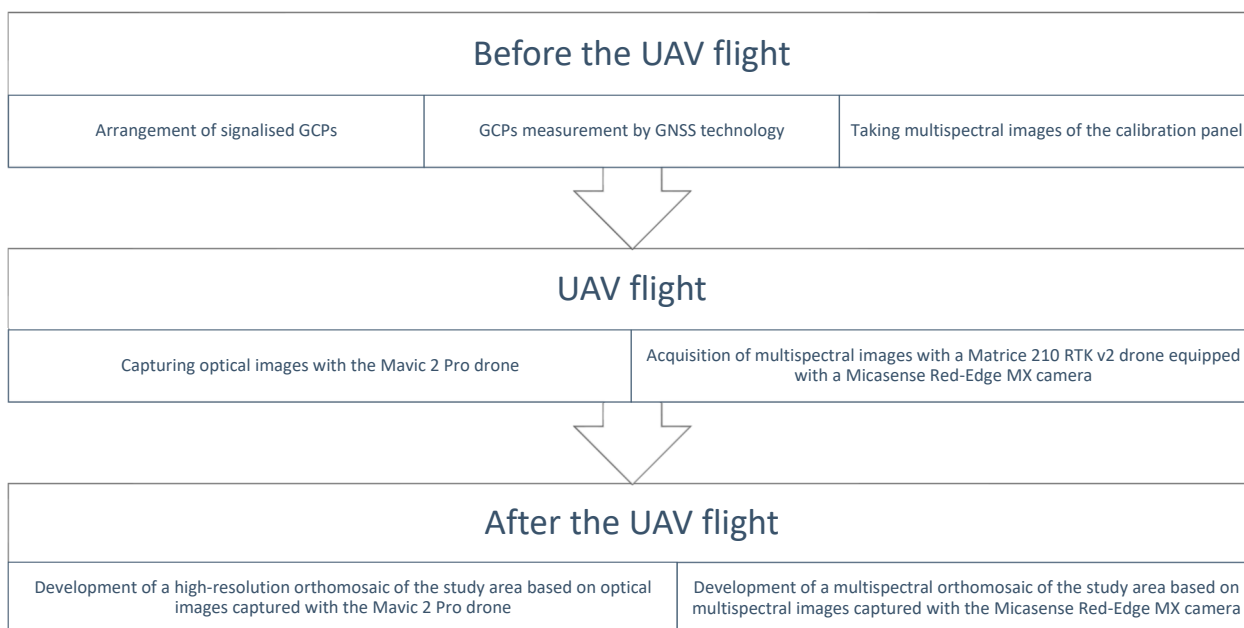


Figure 2. UAV image acquisition workflow.

Before the flight, chequerboard targets were set up to act as ground control points (GCPs) for post-processing of the data. Each target was targeted with Global Navigation Satellite System (GNSS) and Real-Time Kinematic (RTK) techniques using a Topcon HiPer HR satellite receiver and the TPI NetPro network of reference stations. Ground control points were measured in 30 continuous epochs. Flights were carried out using two UAVs: Mavic 2 Pro and Matrice 210 RTK v2. The comparative specifications of the two UAV platforms are presented in Table A1. The acquired images were processed in the Agisoft Metashape software Version 1.8.2.

In order to generate a high-resolution orthomosaic to determine geometric relationships between characteristic points around the bioreactors, images were acquired with a Mavic 2 Pro drone (DJI, China) with a field pixel of 1.8 cm/pix. The forward and cross-sectional overlays a priori were set at 70%. Due to strong wind gusts, the speed of the flying platform during the ongoing mission was set at 3 m/s, which allowed sharp images to be obtained, with a quality image of more than 0.85. The generated orthophoto map was helpful in interpreting multispectral data with a lower spatial resolution.

For the assessment of reflectance and spectral indices, a UAV flight was performed with the Micasense Red-Edge MX (Micasense, WA, USA) multispectral camera. The characteristics of the Micasense Red-Edge MX camera are presented in Table A2 [23]. The UAV platform under which the multispectral sensor was adapted was the UAV Matrice 210 RTK v2. DJI Pilot software was used to create the photogrammetric mission and plan the flight parameters. Due to the high cloud cover during the survey day, in addition to a calibration panel with a white standard, a downwelling light sensor (DLS) was used to determine the ambient irradiance from different directions for each registered channel. The result of the in-camera work was a five-channel multispectral orthomosaic with a field pixel of 4 cm/pix, which was used to conduct further spectral analyses.

3.2. In Situ Measurements

Online measurements of the chemical parameters monitored in the municipal wastewater treatment process, using the example of the analysed WWTP in Poland, were made using specialised metres that allow real-time measurements. In this study, the investigated chemical parameters were ammonium nitrogen ($\text{NH}_4\text{-N}$), phosphates ($\text{PO}_4\text{-P}$), and nitrate nitrogen ($\text{NO}_3\text{-N}$).

For the determination of $\text{NH}_4\text{-N}$, an ATMAX sensor was used with a diluted sample, operating on the basis of a gas-selective electrode (GSE) with a screw-on membrane cap. The ATMAX analyser is used both in influent wastewater—at the beginning of the nitrification stage—and in effluent wastewater. For the measurement of $\text{PO}_4\text{-P}$, the PHOSPHAX orthophosphate analyser was used in this study. It uses a method based on the determination of phosphate concentration using colorimetric analysis with a molybdovanadate reagent. The NITRATAX probe was used to determine $\text{NO}_3\text{-N}$. The spectrophotometric method of this sensor is based on the principle of absorption of electromagnetic radiation from $\text{NO}_3\text{-N}$ and $\text{NO}_2\text{-N}$ compounds at a wavelength of 254 nm [24].

3.3. Spectral Analyzes

The in situ information obtained may not be representative of the entire study area due to the point and too infrequent nature of the observations. This prevents reliable interpolation of the data. The spatial distribution of the analysed parameters is thus more favourable for finding patterns to understand phenomena or explain the occurrence of anomalies. In the literature review, many references can be found to the implementation of methodologies for spatial and temporal analyses based on remote sensing data at different research levels [1,17,19,25]. Among these, spectral analyses based on spectral curves and spectral indices can be distinguished.

The spectral curve expresses the value of the reflectance of electromagnetic radiation with respect to the electromagnetic wavelength. In the case of spectral images taken with radiometric sensors, the DN (Digital Number) pixel values are directly proportional to the physical reflectance value of electromagnetic radiation and can thus be equated with the reflectance of radiation. Depending on the structure of the object being analysed and its physical and nutrient compounds, the reflectance value will vary. This phenomenon allows local anomalies to be identified and radiometric values (or values of calculated spectral indices) to be related to parameters characterising the object or process involved.

There are many spectral indices based on different spectral responses (using different ranges of the electromagnetic radiation spectrum), allowing one to look for relationships between the values of spectral indices and the physical and chemical parameters of interest.

The calculated values of spectral indices can be visualised in the form of a composition of spatial maps of the index distribution with a legend. The research presented here focuses on six commonly used spectral indices that can be determined with the available Micasense Red-Edge MX camera. These indicators are as follows: NDVI, OSAVI, and GNDVI, often cited in studies by other authors [14,16,26], and $\text{NDVI}_{\text{RED-EDGE}}$, $\text{OSAVI}_{\text{RED-EDGE}}$, and $\text{GNDVI}_{\text{RED-EDGE}}$ derivatives of the indices mentioned above. The indicated spectral indices are most commonly used in relation to plant vegetation or the mode of photosynthesis. However, in line with the experience of other authors [15,27], this does not exclude the use of the listed spectral indices for other purposes.

The most recognisable spectral index is the NDVI calculated using Formula (1). It is strongly related to the chlorophyll content of plant leaves and the productivity of biomass [28]. The NDVI index values range from -1 to 1 , which makes it possible to separate areas not covered by vegetation (where photosynthesis does not occur) from areas with dense vegetation and lush condition.

$$\text{NDVI} = \frac{\rho_{\text{NIR}} - \rho_{\text{RED}}}{\rho_{\text{NIR}} + \rho_{\text{RED}}} \quad (1)$$

where ρ_{NIR} is the spectral channel with the recorded reflection of electromagnetic radiation in the near-infrared range ($\sim 0.84 \mu\text{m}$), and ρ_{RED} is the channel recording the red band of optical radiation ($\sim 0.67 \mu\text{m}$).

A modification of the NDVI index that allows even small changes in the plant assimilation apparatus to be taken into account is the OSAVI index. In precision agriculture, it is used at an early stage of crop development when most of the crop is not covered by lush vegetation [26]. Similarly to the NDVI index values, the OSAVI spectral index values are normalised and fall within the range $(-1; 1)$, while 1 represents a high chlorophyll content and strong photosynthesis. The rule of thumb for calculating the OSAVI index value is presented in Formula (2).

$$\text{OSAVI} = \left(\frac{\rho_{\text{NIR}} - \rho_{\text{RED}}}{\rho_{\text{NIR}} + \rho_{\text{RED}} + 0.16} \right) \quad (2)$$

The GNDVI index is used in precision agriculture to estimate photosynthetic rates and to determine the uptake of water and nitrogen by upper levels of plants [17]. Formula (3) describes the calculation of the GNDVI from two spectral channels and is as follows:

$$\text{GNDVI} = \frac{\rho_{\text{NIR}} - \rho_{\text{GREEN}}}{\rho_{\text{NIR}} + \rho_{\text{GREEN}}} \quad (3)$$

where ρ_{GREEN} is the spectral channel with the recorded electromagnetic reflection in the green range ($\sim 0.56 \mu\text{m}$).

For each of the three formulas presented above, modifications can be made by replacing the infrared channel ρ_{NIR} with a red-edge channel $\rho_{\text{RED-EDGE}}$, which allows a more accurate examination of plant health by taking into account not only the crown of the crop but also the lower tiers of the plant.

The limited number of spectral indices presented is due to the small number of spectral channels registered by the Micasense Red-Edge MX camera. In the literature review, no studies on the use of the presented spectral indices were found to assess the performance of WWTPs and analyse the quality of wastewater. Although the spectral indices in question are primarily related to plant monitoring, some researchers [22] have obtained satisfactory results in the analysis of inland waters using the indices cited. Thus, for the purposes of this article, the authors have made the assumption that the values of the indices: NDVI, GNDVI, OSAVI, and derivatives of these indices can be used to monitor the processes occurring in the bioreactor compartments. Each sector of the biological reactor, depending on the aeration situation and the processes taking place in it, had a different chemical

and microbiological composition, which reflected on the microbiological processes on the surface of the reactor sector.

4. Results

The following sections present the results of spectral analyses based on UAV-acquired data and in situ measurements.

4.1. Spatial Maps of Spectral Indices

By visually analysing Figure 3a–f, it is possible to observe the change in the values of the spectral indices analysed between the different thematic compositions. For the NDVI (Figure 3a) and $\text{NDVI}_{\text{RED-EDGE}}$ (Figure 3b) indicator maps, the range of values presented in the legend is similar. Within the nitrification (CN), dephosphatation (CDP), and denitrification (CDN) compartments of the bioreactor analysed, a greater variation in the values of the NDVI, GNDVI, and OSAVI indicators can be seen in Figure 3a,c,e. These maps are more visually contrasting than the derived maps of the listed indices, where successive compartments of the bioreactor are similar with respect to each other. This may indicate that the $\rho_{\text{RED-EDGE}}$ channel recorded by the Micasense Red-Edge MX multispectral camera analysed in this study is not sensitive to changes in the quality of the biomass parameters in the bioreactor compartments.

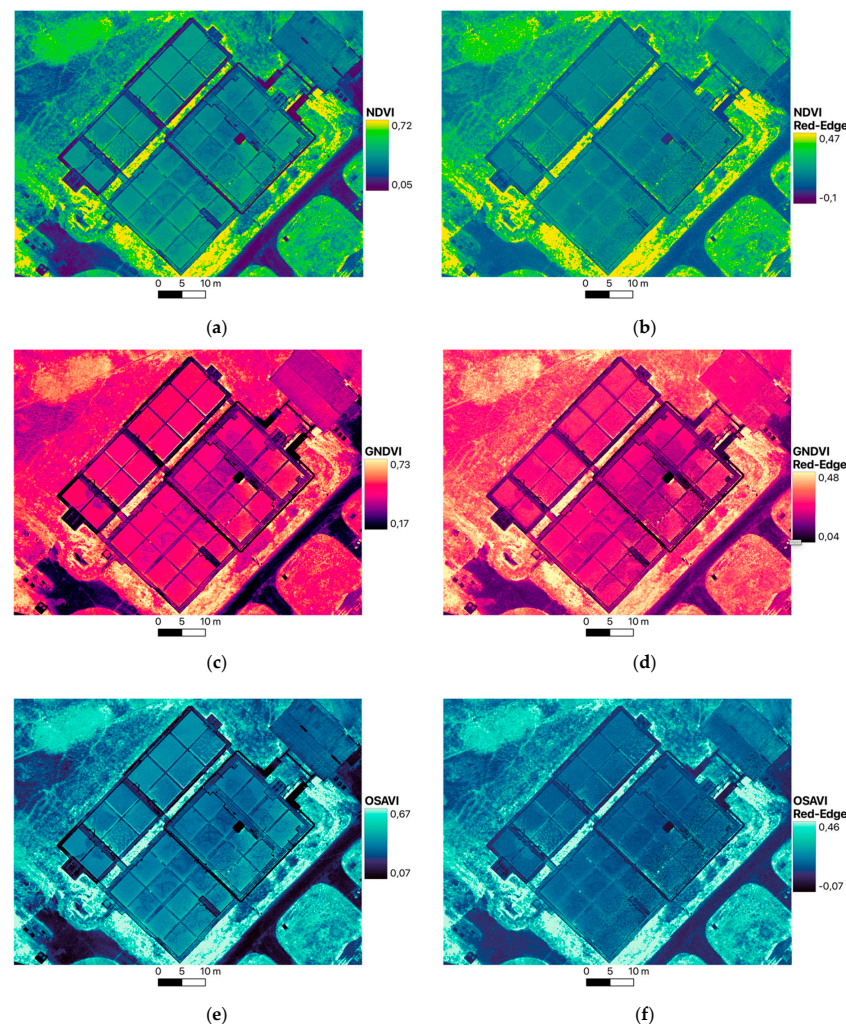


Figure 3. Maps of the spectral indices of biomass in the eastern bioreactor at the WWTP in Stara-chowice (Poland): (a) NDVI index, (b) $\text{NDVI}_{\text{RED-EDGE}}$ index, (c) GNDVI index, (d) $\text{GNDVI}_{\text{RED-EDGE}}$ index, (e) OSAVI index, and (f) $\text{OSAVI}_{\text{RED-EDGE}}$ index.

The search for anomalies in processed remote sensing images usually boils down to the identification of local areas with different radiation characteristics or spectral indices. Areas with anomalies stand out in relation to their surroundings and allow a preliminary qualitative analysis to be carried out. Depending on the degree of aeration of the bioreactor compartments, the texture of the biomass in the map compositions and the high-resolution RGB orthophoto varies. Maps of the spectral indices NDVI (Figure 3a), GNDVI (Figure 3c), and OSAVI (Figure 3e) allowed anomalies to be localised inside some of the CNs, as presented in Figure 4. The area highlighted in red shows two compartments for which a contrast in the values of the spectral indices can be seen. The compartment with the biomass located higher up is more homogeneous in terms of indicator values than the compartment located to its right, where the spread of NDVI, GNDVI, and OSAVI indicator values is much greater. This allows us to conclude that the spectral indices analysed in this paper in the form of NDVI, GNDVI, and OSAVI can be sensitive to changes in the chemical parameters of the biomass in the bioreactor compartments.

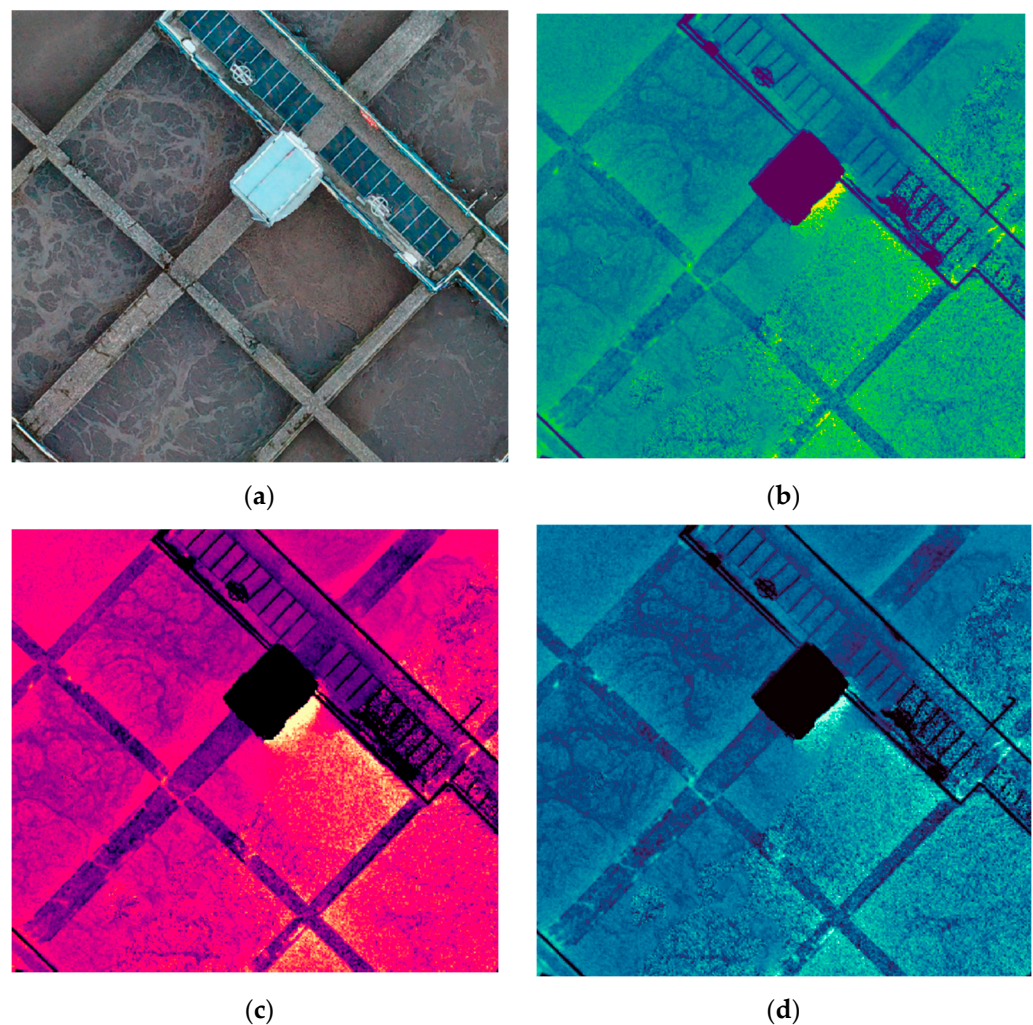


Figure 4. Location of detected anomalies inside the CNs of the bioreactor on a map base: (a) high-resolution orthophoto, (b) NDVI, (c) OSAVI, and (d) GNDVI.

Figure 5 was created to visualise the distribution of the values of the spectral indices analysed for the three compartment types. Within each bioreactor compartment, 200 points were randomly generated, for which the values of the indices from the different map compositions were read, and then the values of the spectral indices were averaged by compartment type. The spectral indices presented have the same value domain, making them possible to present in a single graph.

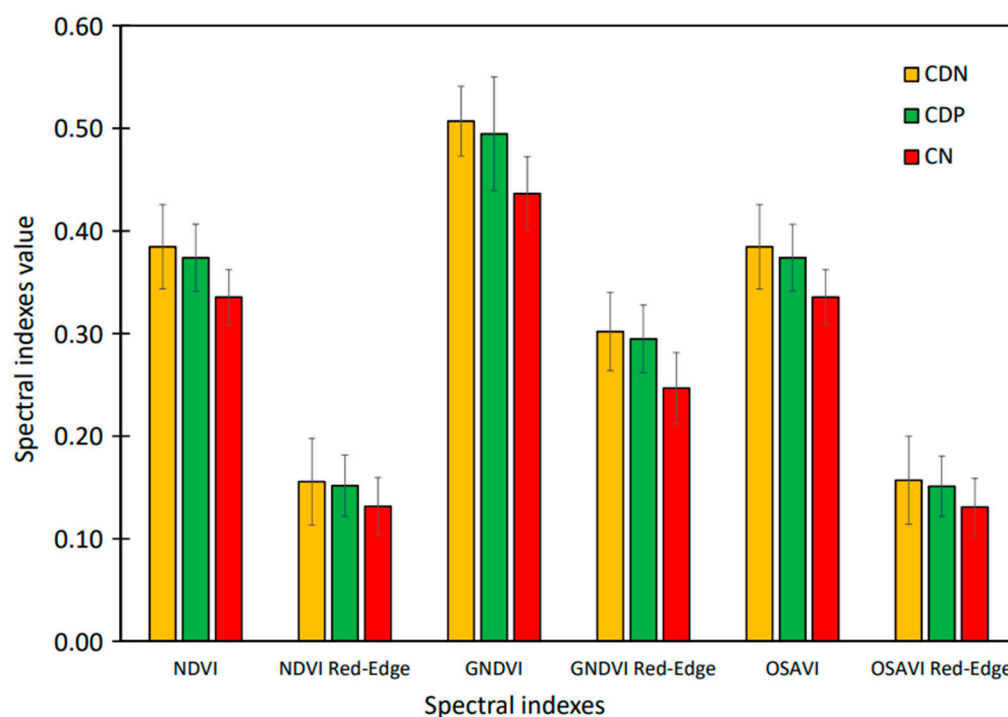


Figure 5. Distribution of the values of the spectral indices for the bioreactor analysed considering the three types of compartments: CDN, CDP, and CN.

For all six spectral indices analysed, a similar trend of index values was observed for the compared types of compartments in the bioreactor. The highest values of all indices were observed for the CDNs, and the lowest for the CNs (Figure 5). The derived indices in the form of $NDVI_{RED-EDGE}$, $OSAVI_{RED-EDGE}$, and $GNDVI_{RED-EDGE}$ have less differentiated values for CDNs and CDPs. The highest peak between the values of the spectral indices was observed for the GNDVI index in the different types of bioreactor compartments.

Differences in the values of the analysed spectral indices for the compartment types in the bioreactor may result from a number of factors. One factor that should be confirmed in further extended studies is the specificity of the predominant microorganisms in each compartment. Differences in the structural structure of the microorganisms found in each compartment may affect the wave reflection, as evidenced by the different values of all indicators. In the case of CN, the dominant ammonium nitrogen oxidising bacteria most extensively studied is *Nitrosomonas europaea* [29]. These bacteria carry out the nitrification process, which requires the presence of appropriate specific enzymes and energy transporters, i.e., ammonium monooxidase, hydroxylamine oxidoreductase, nitrite oxidoreductase, or specific cytochrome c. These proteins are contained in, among others, periplasmic areas of the cytoplasm and also in the very thick—in the case of this bacterium—cell membrane or, importantly, only in the periplasm of the cells of nitrifying bacteria [30], which can directly affect the reflection of radiation and lower results of the obtained indicators (Figure 5) compared to the dominant groups of bacteria in the CDP or CDN. Confirmation from further in-depth research requires knowledge regarding the specificity of microorganisms that dominate in all sectors. Another likely reason for the differences in the values of the analysed spectral indices for the compared types of compartments in the bioreactor is that the amount of organic matter decreased sequentially in the WWTP processes in the activated sludge compartments. These processes involved the mineralisation of organic matter and the formation of humic and fulvic acids [31].

In order to fully summarise the statistics describing the distribution of spectral indices in the bioreactor compartments, a boxplot based on quantiles was created (Figure 6). The greatest scatter in the values of the spectral indices was observed for the CNs and CDNs, which may be due to the activity of biological processes during the acquisition of aerial

photographs. For this reason, the optimum option for acquiring multispectral images from UAVs should be to carry out a UAV flight at a much higher altitude and with fewer images. The values of all spectral indices are most closely grouped with respect to the mean value for the dephosphatation compartment, which was the least variable during the raid in terms of the visual organic matter observed in its top layer. This could be explained by a lower concentration of phosphorus compounds and, consequently, a lower rate of the dephosphatation process.

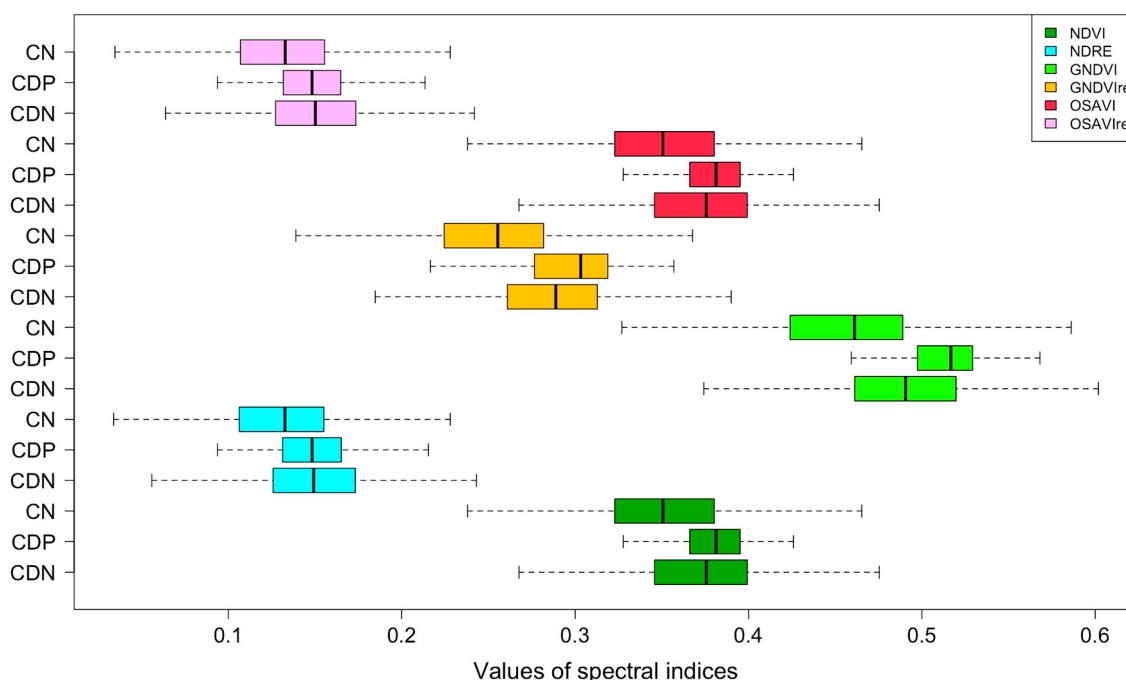


Figure 6. Scatter plot of the analysed spectral indices for the three types (CDN, CDP, and CN) of bioreactor compartments.

4.2. Operating Conditions of the Wastewater Treatment Plant during the Experiment

As the operation of a WWTP requires simultaneous control of multiple processes, a number of measuring devices mounted on its process facilities are used. A desirable situation would be to measure the WQI in the influent and effluent of the treatment plant and correct the bioreactor settings. Currently, most domestic facilities have online monitoring of biological reactor settings [3]. Table 1 presents the results of the online measurements of the bioreactor on the day the experiment was carried out using a UAV.

Table 1. Summary of results obtained for chemical parameters from online measurements for three types of bioreactor compartments in Starachowice.

Wastewater Quality Index	Designation	Dephosphatation Compartment	Denitrification Compartment	Nitrification Compartment
Ammonium nitrogen [mg/L]	NH ₄ -N	25.72	16.46	5.73
Phosphates [mg/L]	PO ₄ -P	48.13	25.86	0.00
Nitrate nitrogen [mg/L]	NO ₃ -N	0.14	0.17	4.35

The above results confirm the high efficiency of removal of biogenic compounds NH₄-N at 78% and PO₄-P at 100%, respectively. At the same time, the results of measurements of nitrogen forms, i.e., NH₄-N or NO₃-N, in the following intervals indicated that nitrification and denitrification in the bioreactor were properly occurring.

4.3. Spectral Analyses

Figure 7 presents the three spectral curves determined from the data acquired by the UAV for the three types of compartments analysed in the bioreactor. The differences obtained between the curves allow the different types of compartments to be distinguished and, thus, the different processes taking place in each compartment to be identified.

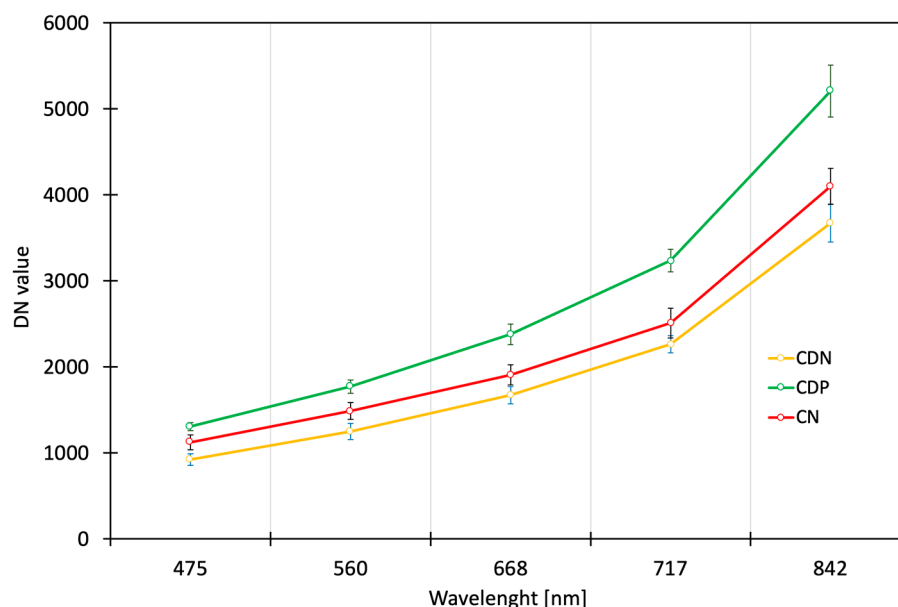
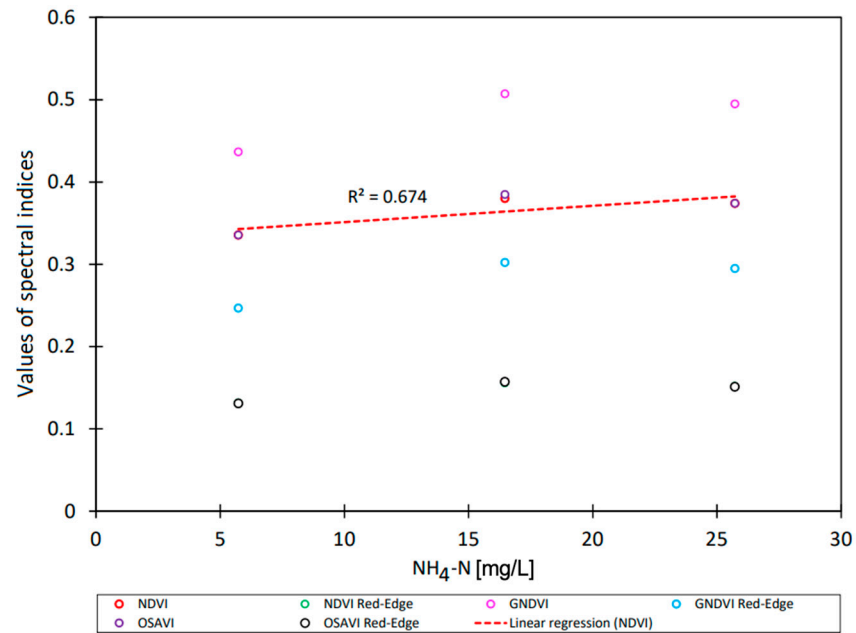


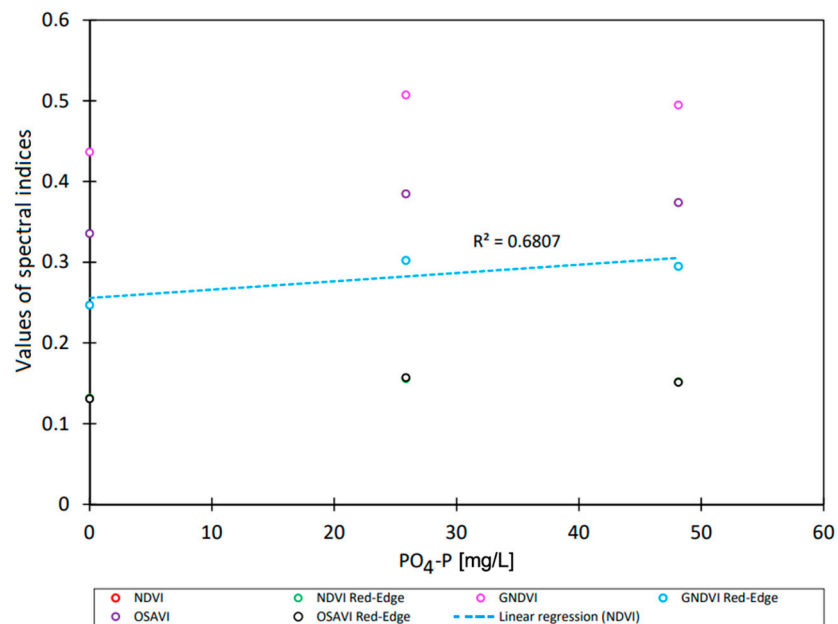
Figure 7. Graphs of the spectral curves for the three compartments analysed in the bioreactor.

Based on Figures 6 and 7, it was found that the biomass accumulated in the different types of compartments of the analyzed bioreactor had different reflectance. In wastewater treatment technologies with simultaneous phosphorus and nitrogen removal, the sludge is subjected to alternating anaerobic, anoxic, and aerobic conditions [32]. As a result, a diverse bacterial flora develops in the biocenosis of activated sludge, capable of increasing phosphorus accumulation in its cells and simultaneously reducing ammonium nitrogen. Under anaerobic conditions, phosphorus is released into the environment as a result of the decomposition of intracellular polyphosphates, and the resulting energy is used by phosphorus bacteria for the biosynthesis of spare substances. Under aerobic conditions, there is rapid uptake of converted and stored dissolved phosphorus to polyphosphates [33–35]. At the same time, Kern-Jaspersen and Henze [36] formulated the hypothesis that two types of phosphorus microorganisms can occur in anaerobic wastewater treatment systems. One type of phosphotrophic bacteria can use only oxygen as an electron acceptor, while the other group can use both oxygen and nitrate. Thus, under different aerobic conditions, different groups of phosphorus bacteria will dominate in the different CDPs, CDPs, and CNs. In the first anaerobic compartment, the denitrification and dephosphatation system will release phosphate into the environment [37]. On the other hand, already under anoxic conditions, a group of bacteria using nitrites and nitrates as electron acceptors in the oxidation of poly- β -hydroxybutyric acid (PHB)—begin to accumulate phosphorus. Two well-known processes then take place, that is, biological dephosphatation and heterotrophic dissimilatory denitrification [38]. The existence of different groups of phosphorus bacteria and, at the same time, their variable activity in accumulating or releasing phosphorus may be the direct reason for the differences between the UAV spectral curves. The reason for the large discrepancy between UAV spectra from CDP and UAV spectra from CDN and CN may have been the activation of phosphorus-accumulating bacteria in the form of polyphosphates already in the anoxic compartment (in CDN). However, these are conjectures, and this study would need to be expanded to include microbiological analyses.

In order to verify this assumption, it was decided to relate the results of the chemical analysis of the effluent to the spectral indices using a simple regression model and then to determine the coefficient of determination R^2 . The results with the highest fit values are presented in Figure 8.



(a)



(b)

Figure 8. Cont.

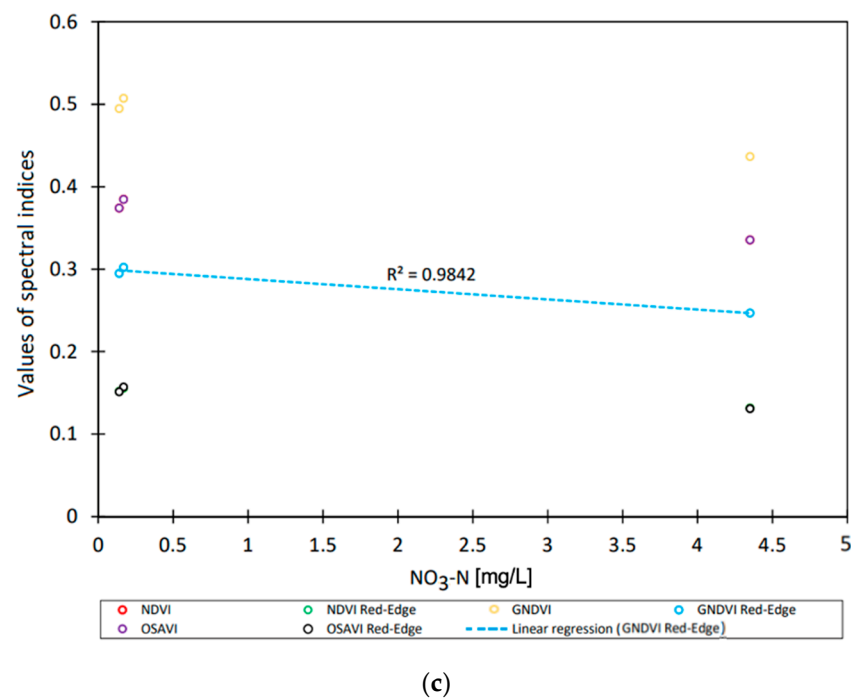


Figure 8. Plots of the dependence of the values of the spectral indices NDVI, OS-AVI, GNDVI, NDVI_{RED-EDGE}, OS-AVI_{RED-EDGE}, and GNDVI_{RED-EDGE} on the effluent quality indices in the forms of (a) ammonium nitrogen, (b) phosphate, and (c) nitrate nitrogen for the analysed bioreactor.

For all three effluent quality indicators, a linear relationship was observed in the values presented in the study of the spectral indices. The strongest correlation was observed for the GNDVI_{RED-EDGE} indicator and NO₃-N, for which the determination index was $R^2 = 0.98$. In the oxygen (nitrification) compartment, ammonia is oxidized to nitrate, and there is an excess uptake of phosphate released in the anaerobic zone. The process occurs primarily with the use of nitrifying bacteria, whose biological membrane structure differs from other groups of bacteria, which may be the reason for the variation of GNDVI_{RED-EDGE} values in the CN. The large disparity between NO₃-N values in biological compartments and the variability of dominant bacterial groups in the different defosfatation, denitrification, and nitrification processes may be the reason for the strong regression between the NO₃-N concentration and the GNDVI_{RED-EDGE} coefficient. This process occurs primarily with the participation of nitrifying bacteria, whose biological membrane structure differs from other groups of bacteria, which may have been the reason for the variation of GNDVI_{RED-EDGE} values in the CN. The proliferation of biomass of bacteria (including filamentous bacteria), protozoa, and invertebrates under aerobic conditions may also affect the reflectance and lower results of the obtained GNDVI_{RED-EDGE} index. However, the small amount of data requires this study to continue to confirm the results obtained.

5. Discussion

The recorded spectral response by the remote sensing detector might have been disturbed by a number of factors, such as illumination of the object from different angles, objects around the object under study (introducing multiple reflections of electromagnetic radiation), or variable atmospheric conditions during multispectral data acquisition. Nevertheless, UAV platforms have more flexibility in selecting optimal conditions for conducting analyses than when working with satellite images, which for the latitude of Poland are often unsuitable for conducting quantitative analyses due to frequent cloud cover occurring in autumn–winter [7,16,17].

The analysis of the obtained spectral indices showed the greatest difference between the results for the nitrification and denitrification compartments (Figures 5 and 6). This

result was confirmed by the data obtained from the measurements at CDN and CN (Table 1). The greatest difference was obtained between the effluent quality indicators tested in the selected compartments for phosphate. In the case of ammonium nitrogen, a decrease in its value was found in CN compared to CDN, indicating the correct course of nitrogen removal from wastewater. As a result of the detailed analysis of spatial maps of spectral indices (Figure 3), it was possible to locate an anomaly inside the CNs of the bioreactor analysed (Figure 4). This might indicate the presence of a large variation in effluent quality within the bioreactor compartments and, consequently, potential problems with its operation in the form of the formation of so-called dead zones. However, the verification of the hypothesis cited requires additional measurements and the creation of a hydrological model of the bioreactor.

Measurements taken with a spectral camera showed differences in electromagnetic reflectance values for the CNs, CDNs, and CDPs, as shown in Figure 8. These results confirmed the data from measurements of selected WQI indicators for the bioreactor compartments (Figure 7). The data showed that the processes taking place in each compartment influence the values of selected WQI indicators. This fact can be used in the construction of the soft sensor, but there is a need to extend the scope of measurement studies using drones and to perform laboratory measurements of selected indicators of wastewater quality. Thus, further research is required.

WWTPs collect a large amount of data that can be used to develop process models to support the operation of the plant. From the point of view of WWTP operation, it was interesting not only to predict the wastewater treatment process but also to simulate it. It is important to use mathematical models to control the processes occurring in the treatment plant, that is, to determine these bioreactor settings to ensure the required effluent quality with the lowest operating costs [4]. The research carried out in this paper demonstrates the potential of UAV technology and multispectral imagery in the context of identifying the operating conditions of WWTPs, and the research findings are in line with the experience of other authors [27,39].

The results obtained showed correlations that can be used at the stage of WWTP operation control, operation, and monitoring of bioreactor performance. The proposed approach can be an alternative to classical solutions (use of online sensors), including those based on developed soft sensors. At present, continuous monitoring is used in many WWTPs, but it is not possible to carry out measurements at the stage of system failure, sensor calibration, replacement, or maintenance. The results obtained (Figure 8) significantly confirm the relationships between the NDVI and $GNDVI_{RED-EDGE}$ spectral indices and ammonium nitrogen (NH_4-N), phosphate (PO_4-P), and nitrate nitrogen (NO_3-N). Presumably, these relationships may have been due to the variable biomass of the dominant groups of organisms in the treatment compartments. In the aeration compartment, these will mainly be nitrifying bacteria, protozoa, and invertebrates [40], which decompose organic matter and contribute to the humus in the sludge, which may be reflected especially in the value of the $GNDVI_{RED-EDGE}$ ratio. The supposition of the influence of biomass variation in compartments on UAV spectral indices was attempted to substantiate with UV-VIS spectra of the phosphorus bacteria *Bacillus megaterium*, where the absorption maximum occurred at 550 nm [41]. In addition, the validity of the conjecture may have been evidenced by the UV-VIS spectra of other microorganisms for which the absorption maxima were in the red wavelength range [42,43]. These conclusions can be used in the operation stage of the treatment plant and may provide a solution for obtaining data on the performance of the bioreactor in emergency situations. The aforementioned correlation showed a strong correlation ($R^2 = 0.98$) between $GNDVI_{RED-EDGE}$ and nitrate nitrogen, which allows the possibility of developing soft sensors. The tools used to create a computational model (in the above case of WQI) from the collected data were used to identify selected indicators of wastewater quality in bioreactor compartments. However, due to the number of experiments carried out, these analyses must be continued in order to confirm the relationships obtained and, on the other hand, collect enough data to determine a computational model.

6. Conclusions

On the basis of the research carried out, it was concluded that it is possible to separate the nitrification, dephosphatation, and denitrification compartments for the bioreactor analysed using the characteristics of the spectral curves. The values analysed of the spectral indices are as follows: NDVI, OSAVI, GNDVI, NDVI_{RED-EDGE}, OSAVI_{RED-EDGE}, and GNDVI_{RED-EDGE} show a linear relationship with respect to the concentrations of ammonia nitrogen, nitrate nitrogen, and phosphate in the analysed bioreactor. However, the small number of observations in this study necessitates the continuation of this study. The research conducted may find application in the construction of a soft sensor for monitoring the operating conditions of a WWTP.

Given the potential of the results obtained, further analyses involving varying operating conditions in the bioreactor (changing inflow, temperature, and quality in the compartments) for different seasons are advisable.

Author Contributions: Conceptualization, B.S.; methodology, S.S. and B.S.; formal analysis, S.S. and B.S.; investigation, S.S. and B.S.; resources, S.S. and B.S.; data curation, S.S., B.S. and R.S.; writing—original draft preparation, S.S., B.S. and R.S.; writing—review and editing, S.S., B.S. and R.S.; visualization, S.S.; supervision, S.S., B.S. and R.S. All authors have read and agreed to the published version of the manuscript.

Funding: The project is supported by the program of the Minister of Science and Higher Education under the name: “Regional Initiative of Excellence”; in 2019–2023 project number 025 / RID / 2018/19 financing amount PLN 12,000,000.

Data Availability Statement: The data presented in this review are available within the text of the article and figures.

Acknowledgments: We would like to thank the Management of the Starachowice Wastewater Treatment Plant and Karol Cienciała (Department of Maintenance, Repairs and Investments, Kielce University of Technology) for allowing us to carry out research at the wastewater treatment plant and for providing access to the measurement results from the bioreactor compartments.

Conflicts of Interest: The authors declare no conflict of interest.

Abbreviations

CDN	Denitrification compartment
CDP	Dephosphatation compartment
CN	Nitrification compartment
DLS	Downwelling Light Sensor
DN	Digital Number
DSM	Digital Surface Model
GCP	Ground Control Points
GNDVI	Green Normalized Difference Vegetation Index
GNSS	Global Navigation Satellite System
GPS	Global Positioning System
GSD	Ground Sample Distance
GSE	Gas-Selective Electrode
NDVI	Normalized Difference Vegetation Index
NH ₄ -N	Ammonium Nitrogen
NO ₃ -N	Nitrate Nitrogen
NUC	Nutrient Content
OSAVI	Optimised Soil Adjusted Vegetation Index
PHB	Poly-β-hydroxybutyric
PO ₄ -P	Phosphate
RTK	Real-Time Kinematic
UAV	Unmanned Aerial Vehicle
WQI	Wastewater Quality Indicator
WWTP	Wastewater Treatment Plant

Appendix A

Table A1. Comparative characteristics of the UAVs used in this study.

Division	Contents for Mavic 2 Pro	Contents for Matrice 210 RTK v2
Weight	0.91 kg	4.90 kg
Flight time on one battery	~25 min	~34 min
IP tightness standards	No	IP43
Possibility to adapt many sensors (e.g., replaceable optics)	No	Yes
RTK corrections	No	Yes

Table A2. Characteristics of the Micasense Red-Edge MX multispectral camera used.

Weight (include DLS 2 system)	231.9 g	
Dimensions	8.7 cm × 5.9 cm × 4.5 cm	
Spectral Bands	Blue, Green, Red, Red edge, Near-IR, 12-bit RAW for each	
Wavelength (nm)	Band 1	Blue—475 nm center, 32 nm bandwidth
	Band 2	Green—560 nm center, 27 nm bandwidth
	Band 3	Red—668 nm center, 14 nm bandwidth
	Band 4	Red edge—717 nm center, 12 nm bandwidth
	Band 5	Near-IR—842 nm center, 57 nm bandwidth
Ground Sample Distance (GSD)	8 cm per pixel (per band) at 120 m AGL	
Field of View	47.2° HFOV	

References

- Kowalik, R.; Latosińska, J.; Gawdzik, J. Risk Analysis of Heavy Metal Accumulation from Sewage Sludge of Selected Wastewater Treatment Plants in Poland. *Water* **2021**, *13*, 2079. [\[CrossRef\]](#)
- Luo, Q.; Chen, L.; Liu, F. Optimization of denitrification treatment of freshwater aquaculture tailwater based on distributed control technology. *Desal. Water Treat.* **2021**, *239*, 19–30. [\[CrossRef\]](#)
- Szeląg, B. *Mathematical Modelling, Optimisation and Control of Flow-Through Wastewater Treatment Plants*, Polish Academy of Sciences; Systems Research Institute: Warsaw, Poland, 2019.
- Wodecka, B.; Drewnowski, J.; Białek, A.; Łazuka, E.; Szulżyk-Cieplak, J. Prediction of Wastewater Quality at a Wastewater Treatment Plant Inlet Using a System Based on Machine Learning Methods. *Processes* **2022**, *10*, 85. [\[CrossRef\]](#)
- Karolinczak, B.; Miłaszewski, R.; Dąbrowski, W. Cost Optimization of Wastewater and Septage Treatment Process. *Energies* **2020**, *13*, 6406. [\[CrossRef\]](#)
- Wojnowska-Baryła, I.; Kulikowska, D.; Bernat, K. Effect of Bio-Based Products on Waste Management. *Sustainability* **2020**, *12*, 2088. [\[CrossRef\]](#)
- Liu, Y.; Zhang, Z.; Li, Y.; Liu, T.; Ye, W.; Weng, S. Monitoring and scheduling of pollution disaster in agricultural waters based on INSAR. *Desal. Water Treat.* **2019**, *149*, 341–351. [\[CrossRef\]](#)
- Carreres-Prieto, D.; García, J.T.; Cerdán-Cartagena, F.; Suardiaz-Muro, J. Wastewater Quality Estimation through Spectrophotometry-Based Statistical Models. *Sensors* **2020**, *20*, 5631. [\[CrossRef\]](#)
- Havlik, I.; Beutel, S.; Scheper, T.; Reardon, K.F. On-Line Monitoring of Biological Parameters in Microalgal Bioprocesses Using Optical Methods. *Energies* **2022**, *15*, 875. [\[CrossRef\]](#)
- Zhang, Z.; Han, Y.; Chen, J.; Cao, Y.; Wang, S.; Wang, G.; Du, N. Fusion rules and image enhancement of unmanned aerial vehicle remote sensing imagery for ecological canal data extraction. *Desal. Water Treat.* **2019**, *166*, 168–179. [\[CrossRef\]](#)
- Martínez, J.S.; Fernández, Y.B.; Leinster, P.; Casado, M.R. Combining Unmanned Aircraft Systems and Image Processing for Wastewater Treatment Plant Asset Inspection. *Remote Sens.* **2020**, *12*, 1461. [\[CrossRef\]](#)
- Zhang, C.; Huang, H.; Li, Y. Analysis of water accumulation in urban street based on DEM generated from LiDAR data. *Desal. Water Treat.* **2018**, *119*, 253–261. [\[CrossRef\]](#)

13. Wong, L.; Vien, B.S.; Ma, Y.; Kuen, T.; Courtney, F.; Kodikara, J.; Chiu, W.K. Remote Monitoring of Floating Covers Using UAV Photogrammetry. *Remote Sens.* **2020**, *12*, 1118. [[CrossRef](#)]
14. Vanegas, F.; Bratanov, D.; Powell, K.; Weiss, J.; Gonzalez, F. A Novel Methodology for Improving Plant Pest Surveillance in Vineyards and Crops Using UAV-Based Hyperspectral and Spatial Data. *Sensors* **2018**, *18*, 260. [[CrossRef](#)] [[PubMed](#)]
15. Yin, F.; Yang, G.; Yan, M.; Xie, Q. Application of multispectral remote sensing technology in water quality monitoring. *Desal. Water Treat.* **2019**, *149*, 363–369. [[CrossRef](#)]
16. Minařík, R.; Langhammer, J. Use of a multispectral UAV photogrammetry for detection and tracking of forest disturbance dynamics. *Int. Arch. Photogramm. Remote Sens. Spat. Inf. Sci.* **2016**, *41*, 711–718. [[CrossRef](#)]
17. Song, B.; Park, K. Detection of Aquatic Plants Using Multispectral UAV Imagery and Vegetation Index. *Remote Sens.* **2020**, *12*, 387. [[CrossRef](#)]
18. Marang, I.; Filippi, P.; Weaver, T.; Evans, B.; Whelan, B.; Bishop, T.; Murad, M.; Al-Shammari, D.; Roth, G. Machine Learning Optimised Hyperspectral Remote Sensing Retrieves Cotton Nitrogen Status. *Remote Sens.* **2021**, *13*, 1428. [[CrossRef](#)]
19. Liu, T.; Liu, X.; Liu, M.; Wu, L. Evaluating Heavy Metal Stress Levels in Rice Based on Remote Sensing Phenology. *Sensors* **2018**, *18*, 860. [[CrossRef](#)] [[PubMed](#)]
20. Wang, F.; Gao, J.; Zha, Y. Hyperspectral sensing of heavy metals in soil and vegetation: Feasibility and challenges. *ISPRS J. Photogramm. Remote Sens.* **2018**, *136*, 73–84. [[CrossRef](#)]
21. Sobura, S.; Hejmanowska, B.; Widlak, M.; Muszyńska, J. The Application of Remote Sensing Techniques and Spectral Analyzes to Assess the Content of Heavy Metals in Soil—A Case Study of Barania Góra Reserve, Poland. *Geomat. Environ. Eng.* **2022**, *16*, 187–213. [[CrossRef](#)]
22. Osińska-Skotak, K. *Methodology for the Use of Super- and Hyperspectral Satellite Data in the Analysis of Inland Water Quality*; Publishing House of the Warsaw University of Technology: Warsaw, Poland, 2010.
23. Micasense Producer Website. Available online: <https://support.micasense.com> (accessed on 26 November 2022).
24. Internet Website. Available online: <https://pl.hach.com> (accessed on 6 January 2022).
25. Valenti, F.; Toscano, A. A GIS-Based Model to Assess the Potential of Wastewater Treatment Plants for Enhancing Bioenergy Production within the Context of the Water-Energy Nexus. *Energies* **2021**, *14*, 2838. [[CrossRef](#)]
26. Jełowicki, Ł.; Sosnowicz, K.; Ostrowski, W.; Osińska-Skotak, K.; Bakula, K. Evaluation of Rapeseed Winter Crop Damage Using UAV-Based Multispectral Imagery. *Remote Sens.* **2020**, *12*, 2618. [[CrossRef](#)]
27. Asgharnejad, H.; Sarrafzadeh, M.H. Development of Digital Image Processing as an Innovative Method for Activated Sludge Biomass Quantification. *Front. Microbiol.* **2020**, *11*, 574966. [[CrossRef](#)]
28. Polykretis, C.; Grillakis, M.G.; Alexakis, D.D. Exploring the Impact of Various Spectral Indices on Land Cover Change Detection Using Change Vector Analysis: A Case Study of Crete Island, Greece. *Remote Sens.* **2020**, *12*, 319. [[CrossRef](#)]
29. Zhao, Z.; Luo, J.; Jin, B.; Zhang, J.; Li, B.; Ma, B.; An, X.; Zhang, S.; Shan, B. Analysis of Bacterial Communities in Partial Nitrification and Conventional Nitrification Systems for Nitrogen Removal. *Sci. Rep.* **2018**, *8*, 12930. [[CrossRef](#)]
30. Chawley, P.; Jagadevan, S.; Yadav, K. Nitrogenous Wastes and Its Efficient Treatment in Wastewater. In *Water Pollution and Management Practices*; Springer: Berlin/Heidelberg, Germany, 2021; pp. 147–175.
31. Anielak, A.; Kryłów, M.; Łomińska-Płatek, D. Characterization of fulvic acids contained in municipal sewage purified with activated sludge. *Arch. Environ. Prot.* **2018**, *44*, 70–76.
32. Zubrowska-Sudoł, M.; Walczak, J. Effects of mechanical disintegration of activated sludge on the activity of nitrifying and denitrifying bacteria and phosphorus accumulating organisms. *Water Res.* **2014**, *61*, 200–209. [[CrossRef](#)] [[PubMed](#)]
33. Di Capua, F.; de Sario, S.; Ferraro, A.; Petrella, A.; Race, M.; Pirozzi, F.; Fratino, U.; Spasiano, D. Phosphorous removal and recovery from urban wastewater: Current practices and new directions. *Sci. Total Environ.* **2022**, *823*, 153750. [[CrossRef](#)] [[PubMed](#)]
34. Li, W.; Sun, H.Z.; Wei, W.; Liu, J.; Fu, J.X.; Wang, J. Study on Denitrifying Dephosphatation Process, Influence Factors and Mechanism. In *Proceedings of the Conference Series: Earth and Environmental Science, 3rd International Conference on Water Resource and Environment (WRE 2017), Qingdao, China, 26–29 June 2017; Volume 82.* [[CrossRef](#)]
35. Sun, L.; Qian, Y.H. Advance of research on denitrifying phosphorus accumulating organisms. *Water Sav. Irrig.* **2015**, *2*, 40–44.
36. Kerrn-Jespersen, J.; Henze, M. Biological phosphorus uptake under anoxic and aerobic conditions. *Water Res.* **1993**, *27*, 617–624. [[CrossRef](#)]
37. Zubrowska-Sudoł, M.; Cyganecka, A. Denitrifying dephosphatation as an alternative solution for nutrient removal from wastewater. *Biotechnologia* **2008**, *1*, 136–145.
38. Zeng, R.J.; Saunders, A.M.; Yuan, Z.; Blackall, L.; Keller, J. Identification and Comparison of Aerobic and Denitrifying Polyphosphate-Accumulating Organisms. *Biotechnol. Bioeng.* **2002**, *83*, 140–148. [[CrossRef](#)] [[PubMed](#)]
39. Widlak, M.; Kowalik, R.; Sobura, S. Quality of the soil and water environment in the immediate vicinity of the Barania Góra Forest Reserve. *Desal. Water Treat.* **2021**, *232*, 404–413. [[CrossRef](#)]
40. Esteban, G.; Téllez, C.; Bautista, L.M. Dynamics of ciliated protozoa communities in activated-sludge process. *Water Res.* **1991**, *25*, 967–972. [[CrossRef](#)]
41. Wyciszkievicz, M.; Saeid, A.; Chojnacka, K.; Górecki, H. Use of *Bacillus megaterium* in solubilization of phosphorus. *Przem. Chem.* **2012**, *91*, 837–840.

42. Kiefer, J.; Ebel, N.; Schlucker, E.; Leipertza, A. Characterization of Escherichia coli suspensions using UV/Vis/NIR absorption spectroscopy. *Anal. Methods* **2010**, *2*, 123–128. [[CrossRef](#)]
43. Kandasamy, K.; Jannatin, M.; Chen, Y. Rapid Detection of Pathogenic Bacteria by the Naked Eye. *Biosensors* **2021**, *11*, 317. [[CrossRef](#)]

Disclaimer/Publisher’s Note: The statements, opinions and data contained in all publications are solely those of the individual author(s) and contributor(s) and not of MDPI and/or the editor(s). MDPI and/or the editor(s) disclaim responsibility for any injury to people or property resulting from any ideas, methods, instructions or products referred to in the content.